www.czasopisma.pan.pl PAN POLSKA AKADEMIA NAUK www.journals.pan.pl

Arch. Metall. Mater. **70** (2025), 4, 1727-1732

DOI: https://doi.org/10.24425/amm.2025.156254

R. MOHAMED[1,2], M.M. AL BAKRI ABDULLAH[1,2*], R.A. RAZAK[1,3], D.L. CH. HAO[1,3], P. AROKIASAMY[1,2], N.A. YAACOB[1,2], MD A.O. MYDIN[4]

HEAT EVOLUTION ANALYSIS FOR DETERMINATION OF NUCLEATION KINETICS OF ALKALI ACTIVATED SLAG

This study investigates the nucleation mechanism of slag alkali activation at different solid-to-liquid ratios, focusing on kinetics, including growth rates. Heat evolution during activation was monitored, and calorimetric data were analyzed using the Johnson-Mehl-Avrami-Kolmogorov model. Compressive strength and phase evolution (via wide-angle X-ray scattering) were correlated with heat evolution to enhance understanding of reaction mechanisms in alkali-activated material formation. This is essential for producing alkali-activated slag that meets standard requirements for construction applications. Results showed the highest heat evolved (–360.60 J/g) did not correlate with the best strength performance (22.69 MPa at 1 day and 25.83 MPa at 3 days) since the lowest cumulative heat (–226.15 J/g) at an S/L ratio of 1.4 yielded the best strength. This was supported by the highest growth rate (0.1172 min^{-1}) at this ratio. JMAK analysis indicated instantaneous nucleation with one-dimensional rod-like growth, driven by increased nucleation site availability. From the results obtained, it can be concluded that increment in S/L ratio significantly led to increasing nucleation and polymerization of alkali-activated slag thus causing hindering of heat flow proven from the lowest total cumulative heat evolved obtained. In addition, the highest growth rate observed also linearly correspond to the compressive strength observed thus further prove that this ratio indeed being densified by the polymeric gels of alkali-activated slag formed.

Keywords: Heat evolution; nucleation mechanism; growth rate; alkali-activated slag and compressive strength

1. Introduction

The increasing demand for sustainable construction materials has intensified research into alternatives to ordinary Portland cement (OPC), which is a significant contributor to global CO_2 emissions. Alkali-activated materials (AAMs) in which including geopolymers have emerged as viable eco-friendly binders due to their ability to utilize industrial by-products such as ground granulated blast furnace slag (GGBFS) and fly ash, reducing the environmental footprint while maintaining or exceeding the mechanical properties of OPC [1,2]. Among these, alkali-activated slag (alkali-activated slag) systems are particularly attractive due to their high calcium content, rapid setting time [3], and excellent mechanical performance [4], making them suitable for various application. Given its potential as a material for construction, it is essential to further investigate its reaction mechanism on alkali activation process, particularly when optimizing its mix design to achieve superior qualities for specific applications.

The alkali activation of slag involves complex chemical reactions, including the dissolution of precursors, nucleation and polymerization, and reorganization of hydration products. These reactions are highly dependent on several influencing factors, such as the solid-to-liquid (S/L) ratio, molarity of alkali solution utilized and alkali activator ratio. Among these influencing factors, the S/L ratio can be denoted as the most significant, as it directly controls the chemical composition of the alkali-activated slag produced. One of the key approaches to understanding these mechanisms can be found via the analysis of heat evolution during the activation process. Isothermal calorimetry is widely employed for this purpose, as it allows for the real-time monitoring of heat flow associated with exothermic reactions, providing insights into the reaction kinetics and phase transitions [5]. Furthermore, it was determined that the chemical composition of the materials used as AAMs precursors significantly influenced the heat evolution, regardless of the type of materials used. The chemical composition of the materials was

[1] UNIVERSITI MALAYSIA PERLIS (UNIMAP), CENTRE OF EXCELLENCE GEOPOLYMER & GREEN TECHNOLOGY (CEGEOGTECH), PERLIS, MALAYSIA
[2] UNIVERSITI MALAYSIA PERLIS (UNIMAP), FACULTY OF CHEMICAL ENGINEERING &TECHNOLOGY, PERLIS, MALAYSIA
[3] UNIVERSITI MALAYSIA PERLIS (UNIMAP), FACULTY OF CIVIL ENGINEERING &TECHNOLOGY, PERLIS, MALAYSIA
[4] UNIVERSITI SAINS MALAYSIA, SCHOOL OF HOUSING, BUILDING AND PLANNING, GELUGOR 11800, PENANG, MALAYSIA
* Corresponding author: mustafa_albakri@unimap.edu.my

also significantly influenced by the source of the materials. This was proven from the past research on monitoring alkali activation of fly ash [6], metakaolin [7] and slag [8].

In addition, most of the past researches further utilized the calorimetric data obtained for the reaction kinetics analysis. For this purpose, the Johnson-Mehl-Avrami-Kolmogorov (JMAK) model has been extensively applied to evaluate the nucleation and growth behavior specifically involving phase transition such as crystallization and solidification. This model enables the quantification of parameters such as the nucleation, growth dimensionality, and reaction rate, offering a robust framework for characterizing the crystallization and hardening processes. By applying the JMAK model in AAMs field, this model will be beneficial for interpreting the nucleation kinetics of alkali-activated slag by utilizing the heat evolution data focusing on early ages development of the alkali-activated slag and correlating to the excellent properties of the alkali-activated slag that are commonly reported by past researches including its excellent compressive strength and fast hardening.

This study focuses on investigating the influence of varying S/L ratios on the heat evolution and nucleation kinetics of alkali-activated slag. The heat flow data, analyzed through the JMAK model, provides valuable insights into the nucleation mechanisms, growth rates, and phase formation during the alkali activation process. These findings are expected to contribute to the optimization of alkali-activated slag system specifically on improving their compressive strength, durability, and potential for large-scale implementation in sustainable construction practices.

2. Experimental

2.1. Materials and mixing design

In this study, ground granulated blast furnace slag was utilized as solid precursor due to the promising properties reported by past researches. In term of chemical composition, it was found that the slag utilized in this study is mainly composed calcium oxide (CaO), silicon dioxide (SiO_2), aluminium dioxide (Al_2O_3). The slag consists of more than 50% of calcium oxide (CaO) and followed by 25.60% of silicon dioxide (SiO_2) and 10.90% aluminium oxide (Al_2O_3). Alongside the molar ratio of SiO_2/Al_2O_3 of the chemical composition is 2.3 which is significant for polymeric networks of AAMs formation, it is believed that this slag is potential to be utilized as precursor of alkali-activated materials (AAMs) since it has molar ratio of $CaO/(SiO_2+Al_2O_3)$ 1.5 in which is greater than 1 [9].

Meanwhile, sodium hydroxide (NaOH) and sodium silicate solution (Na_2SiO_3) were employed as liquid precursors. Alkali-activated ground granulated blast furnace slag (referred as alkali-activated slag as there is no other slag utilized in this work) was synthesized by combining solid and liquid precursors in accordance with the designated mixing ratios. Three influencing parameters are considered: solid-to-liquid ratios (S/L ratio), molarity of sodium hydroxide, and alkali activator ratios (Na_2SiO_3: NaOH). For emphasis on the impact of varying S/L ratios, the molarity of NaOH and the Na_2SiO_3: NaOH ratio were maintained at 8M and 2.0, respectively. Simultaneously, S/L ratios were adjusted within the range of 0.6 to 1.4.

3. Testing procedure

3.1. Heat evolution determination

The heat flow calorimeter was employed to monitor the heat evolution of alkali-activated slag under isothermal conditions at 27°C (ambient temperature). "ToniCAL, Toni Technik" calorimeter in which was located at the Non-Destructive Test Laboratory, Faculty of Civil Engineering Technology, Universiti Teknologi Mara was utilized. This testing method is in line with the standard specification of standard practice for measuring hydration kinetics of hydraulic cementitious mixtures using isothermal calorimetry (ASTM C1679) and standard test method for measurement of heat of hydration of hydraulic cementitious materials using isothermal conduction calorimetry (ASTM C1702). In this research, external mixing technique to ensure the homogeneity of the mixture throughout the test duration. Approximately 15 grams of freshly prepared AAM paste from each mix design was placed into the sample ampoule, after which the data collection system began recording output voltage and calculating the heat flow over the monitoring period. The heat evolution rate, dQ/dt (J/gh), and the total heat of hydration, $Q(t)$ (J/g), were measured over 72 hours, corresponding to the hydration monitoring period for OPC.

3.2. Nucleation kinetics determination

The total cumulative heat was further utilized for degree of reaction and applied on determining the nucleation growth mechanism during alkali activation of slag. In this study, Johnson Mehl Avrami Kolmogrov model or also known as JMAK Model was used elucidate the nucleation and growth mechanism. The degree of reaction of alkali activation of slag was calculated by using the Schutter technique [10] with the equation provided in Eq. (1).

$$\alpha = \frac{Q(t)}{Q_{\max}} \tag{1}$$

The variable $Q(t)$ represents the heat released that was computed at a given time, whereas $Q_{\max}$ is the overall heat accumulated during the process. It is important to note that the α values were determined during the heat evolution measurement to indicate reaction completeness. Meanwhile, a linear graph of $y = mX + C$ was plotted accordingly as in Eq. (3.3), where $y = \ln[-\ln(1-\alpha)]$, $x = \ln t$. The degree of reaction, α calculated was used to replace the Xc in the equation thus making the equation to be written as in Eq. (2). The nucleation mechanism

exponent (n) is represented by the slope of the straight line, while the growth rate (k) of JMAK is determined by the y-intercept of the straight line.

$$\ln\left[-\ln(1-\alpha)\right] = \ln K + n \ln t \quad (2)$$

3.3. Compressive strength and phase evolution determination

The compressive strength test was performed following ASTM C109 standards, using a Universal Testing Machine (UTM), UH-1000 kN, at a loading rate of 0.6 N/mm^2/s. Fresh pastes from each mix design were cast into 50 mm^3 cubic molds and cured at ambient temperature until the desired testing age. Compressive strength measurements were taken at 1-day and 3-day intervals, corresponding to the heat evolution duration. To further investigate the factors contributing to the highest compressive strength, phase evolution during the hardening of alkali-activated slag was analyzed. For this purpose, 2 g of ground granulated blast furnace slag was mixed with the alkali activator and applied to a Kapton® film in the WAXS sample container. Measurements were conducted using 4-bromobenzoic acid as the standard, a CCD detector, a sample-to-detector distance (SDD) of 89 cm, and an energy level of 9 keV. The resulting Wide-Angle X-ray Scattering (WAXS) profiles were collected as two-dimensional (2D) scattering intensity maps, which were transformed into I-vs.-q curves and displayed as I-vs.-2θ patterns for phase analysis. The X-ray scattering profiles were preprocessed using the SAXSITS program to ensure accurate results.

4. Results and discussions

4.1. Heat evolution analysis

The calorimetric data obtained on the heat evolution of alkali activation slag at different solid-to-liquid ratios (S/L ratios) of 0.6, 0.8, 1.0, 1.2 and 1.4 are presented as in Fig. 1. According to Fig. 1, the initial response peak (Peak I) was seen to occur immediately at the beginning of heat evolution monitoring, within a timeframe of ten hours for all S/L ratios applied. It was found that the intensity of the peak was varied with the variation of S/L ratios applied. Generally, this first significant peak which is commonly observed in heat evolution of alkali-activated materials (AAMs) is known as wetting and dissolution reaction of alkali activation [11]. The occurrence of this peak involves physicochemical reaction of breaking down the aluminosilicate covalent bonds of slag particles for monomers formation. Therefore, the peak started to shift to the left suggesting the reaction process became rapid with increasing S/L ratios applied.

When the S/L ratio was increased to 1.4, the initial peak further shifted to the left, and its maximum intensity decreased, as observed in Fig. 1. This phenomenon can be attributed to the abundance of slag particles, which facilitated rapid dissolution and nucleation during the alkali activation process. However, this accelerated process also led to the saturation of monomers, oligomers, and polymers within the alkali-activated slag gel matrix, which hindered heat flow due to the accumulation of reaction products. Beyond the initial peak, the impact of S/L ratio became more pronounced, particularly in the formation of a broad hump representing the second peak (Peak II), which is consistent with prior study findings [11,12]. Higher S/L ratios resulted in a more pronounced broad hump, with a slight leftward shift, indicative of accelerated nucleation and polymerization processes. In contrast, for an S/L ratio of 0.6, this broad hump was less prominent, suggesting slower reaction kinetics due to the limited availability of slag particles, thereby prolonging the nucleation and polymerization stages.

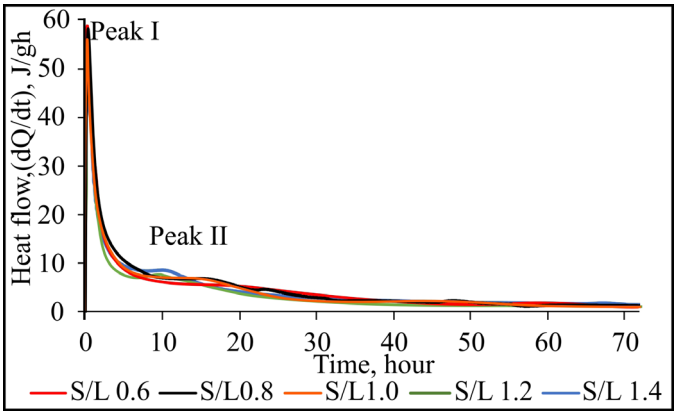

Fig. 1. Heat Evolution of Alkali-activated Slag with different S/L ratios applied

Apart from heat evolution, the total cumulative heat evolved of these heat evolution peaks of alkali activation slag with various S/L ratios applied were also extracted and can be tabulated as in TABLE 1. From TABLE 1, it is believed that the reduction of total cumulative heat evolved is likely attributed to an increase in slag particles, which correlates with higher calcium content. During the dissolution process, covalent bonds within slag particles are disrupted, governed by the reactivity of their chemical composition. As the S/L ratio increases, the molar ratio of CaO/SiO_2 rises, potentially accelerating the dissolution of key monomers essential for nucleation and polymerization, thereby releasing more heat during alkali activation. Furthermore, the elevated CaO content is hypothesized to react with byproducts, such as water (H_2O), from the dissolution process to form calcium-hydrated products, contributing to the observed cumulative heat evolution [13]. However, with the speed up of reaction with increasing molar ratio of CaO/SiO_2, the accumulation of oligomers and hydrated products formed will led to hindering of the heat flow thus causing decreasing in total cumulative heat evolved obtained as being summarized in TABLE 1.

Increasing in S/L ratio is believed to contribute increasing in total cumulative heat evolved during alkali activation due to increasing calcium hydration process which releases more heat as being discussed by most of the past researches [14-16].

TABLE 1

Total Cumulative Heat Evolved

S/L Ratio	Total cumulative heat evolved, J/g
0.6	360.60
0.8	302.45
1.0	297.36
1.2	246.78
1.4	226.15

Although higher calcium content promotes greater heat release due to hydration reactions, the isothermal conditions of the closed alkali-activated slag system in this study suggest that a portion of the evolved heat may be utilized as an energy source for the formation of polymeric networks. This could explain the observed reduction in the total cumulative heat evolved during Peak II with increasing S/L ratios in TABLE 1. Therefore, it can be inferred that the heat released during the alkali activation process plays a significant role in facilitating polymeric network formation, ultimately resulting in a decrease in cumulative heat as the S/L ratio increases.

4.2. Nucleation kinetics analysis

For analysis on nucleation kinetics, degree of reaction analysis is vital in which can be illustrated as in Fig. 2. As being depicted by Fig. 2, rapid development was observed during the first ten hours of reaction for all S/L ratios applied. At 10 hours of reaction in which covers the formation of the first significant peak (Peak I), the highest degree of reaction was found with S/L ratio of 1.4 (0.549) and the lowest was obtained with S/L ratio of 0.6 (0.438). This is can be surmised that S/L ratio leads to faster nucleation and polymerization of the alkali-activated slag due to more availability of slag particles. This will lead to speed up the nucleation and polymerization of the monomers thus leading to decreasing heat evolved as most of the heat was hindered and utilized by the polymeric bond's formation.

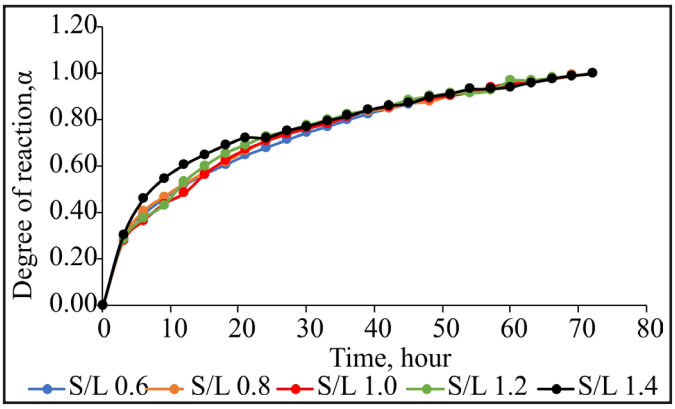

Fig. 2. Degree of Reaction of Alkali-activated Slag

In addition, according to Fig. 2, the degree of reaction continued to develop between 10 and 30 hours of reaction time. During this period, the degree of reaction exceeded 0.700 for all S/L ratios. At 30 hours, the highest degree of reaction (0.778) was recorded at an S/L ratio of 1.4, while the lowest value (0.745) was observed at an S/L ratio of 0.6. Nevertheless, compared to the rapid development observed at 10 hours, the increase in the degree of reaction during this period was noticeably slower for all S/L ratios applied. This phase is thought to involve further polymerization and the reorganization of alkali-activated slag polymeric networks into more stable arrangements, which aligns with the broad hump observed in the heat evolution data rather than a sharp peak. As a result, only a slight increase in the degree of reaction was observed from Fig. 2 during this period. Beyond 30 hours, the degree of reaction across all S/L ratios reached a plateau, remaining stable up to 72 hours. This behavior confirms that the majority of reactions during alkali activation occur rapidly within the first 30 hours. The observed trends are consistent with prior studies, which emphasize the significant influence of external factors on the degree of reaction [17].

Meanwhile, a Johnson-Mehl Avrami Kolmogrov (JMAK) plot of $\ln[-\ln(1-\alpha)]$ vs $\ln t$ was plotted for each of the S/L ratios by utilizing the degree of reaction obtained and the results can be presented as in Fig. 3. From the plot, nucleation mechanism (n) and growth rate (k) value which are exponent of JMAK model was extracted and summarized as in TABLE 2. As can be observed from TABLE 2, the values of n that represent the nucleation type range between 0.8422 and 0.8792, whereas the values of k that were obtained from the y-intercept of the graphs range between 0.0945 and 0.1172 hr^{-1}.

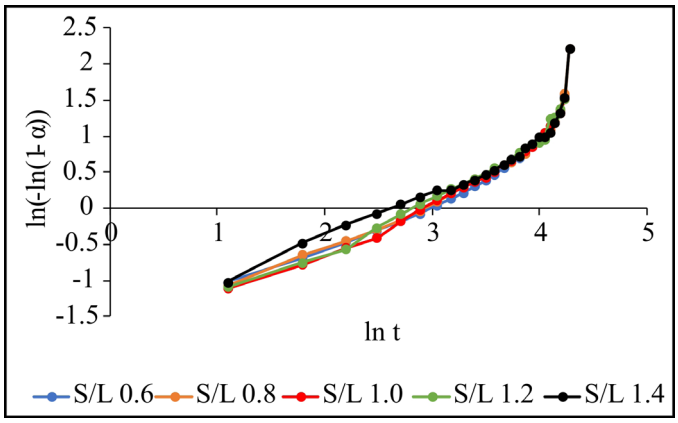

Fig. 3. Johnson Mehl Avrami Kolmogrov model plot of Alkali-activated Slag

From the n values which are more than 0.5 and approaching $n = 1$ in TABLE 2, it can be deduced that the nucleation growth mechanism of alkali-activated slag is same regardless of different S/L ratios applied. The n values indicate that the alkali activation of slag in this study is governed by an instantaneous nucleation mechanism (one-dimensional) characterized by rod-like or needle-like growth. This mechanism implies that alkali activation occurs simultaneously across all transforming regions within the system. As noted in previous studies, the transforma-

tion process eventually slows down as it nears completion due to the depletion of transformable material and the impingement of growing grains [18].

TABLE 2

Extraction of JMAK plot

S/L Ratio	$\ln[-\ln(1-\alpha)] = n\ln t + \ln k$ ($y = mX + C$)	Nucleation mechanism, n	Growth rate, k (hr^{-1})
0.6	$y = 0.8792x - 2.3595$	0.8792	0.0945
0.8	$y = 0.8422x - 2.3532$	0.8422	0.0950
1.0	$y = 0.8700x - 2.3473$	0.8700	0.0956
1.2	$y = 0.8645x - 2.3047$	0.8645	0.0998
1.4	$y = 0.8462x - 2.1438$	0.8462	0.1172

This phenomenon is consistent with the gradual development of the reaction degree for periods beyond 30 hours, as demonstrated. In term of the n values which is less than 1 obtained, it indicates the alkali activation process does not occur at a constant radial growth [19]. Therefore, the development of nucleation was found to be random thus causing the fluctuation to the n values obtained regardless of different S/L ratios applied but still occurred within the same type of nucleation. In term of growth rate which was extracted from the y-intercept (k values), it was found that increasing in S/L ratios led to increasing the growth rate observed from TABLE 2 thus confirming the saturation of alkali-activated slag system with polymerized products could cause reduction in the heat flow due to accumulation in the system. Therefore, the highest growth rate was observed at S/L ratio of 1.4 (0.1172 hr^{-1}) and the lowest was at S/L ratio of 0.6 (0.0945 hr^{-1}).

4.3. Compressive strength and phase evolution analysis

The compressive strength performance for 1-day age and 3-day age can be illustrated as in Fig. 4. According to Fig. 4, the highest compressive strength was found at S/L ratio of 1.4 for both 1-day and 3-day ages (22.69 MPa and 25.83 MPa respectively). The rapid increase in compressive strength of 1-day age is attributed to the rapid formation of calcium-hydrated products including calcium aluminate silicate hydrates gels (CASH) and calcium silicate hydrates gels (CSH) in which is believed to increase the densification of the alkali-activated slag. This phenomenon is also consistent with the highest growth rate obtained. The resulted calcium products from reaction with monomers as well as excess water contributes to strength performance as being mentioned by past researches [13,20]. This was further supported by the reduction of total cumulative heat evolved obtained as being summarized from TABLE 1 in which suggesting is significant for providing energy towards formation of alkali-activated slag gels thus contributing to potential of self-curing.

Furthermore, the rapid formation of calcium-hydrated products, which contributed to the highest compressive strength at an S/L ratio of 1.4, was confirmed by phase evolution observed during the setting of the alkali-activated slag, as shown in Fig. 4. The primary peaks detected in the diffractogram within the 2-theta range of 10°-50° indicate the development of calcium-hydrated products as majority of the phases within these range are calcite, CSH and gismondine, with increasing peak intensity reflecting their development in the alkali-activated slag system.

In addition, as illustrated in Fig. 3, a further development of compressive strength was observed at 3-days age, indicating the strength performance after completion of heat evolution. The highest compressive strength was recorded at an S/L ratio of 1.4, while the lowest was at an S/L ratio of 0.6 (25.83 MPa and 10.07 MPa, respectively). Despite the absence of Peak III in the heat evolution in which was claimed to be a reorganization and reorientation phase, the alkali-activated slag continued to develop in its strength with increasing S/L ratios, suggesting that the reorganization and reorientation of polymeric networks into a more stable arrangement released less heat as the alkali-activated system became compact. The high compressive strength achieved at S/L ratio 1.4 further supports the notion that the densification of the polymeric network hinders heat flow, re-

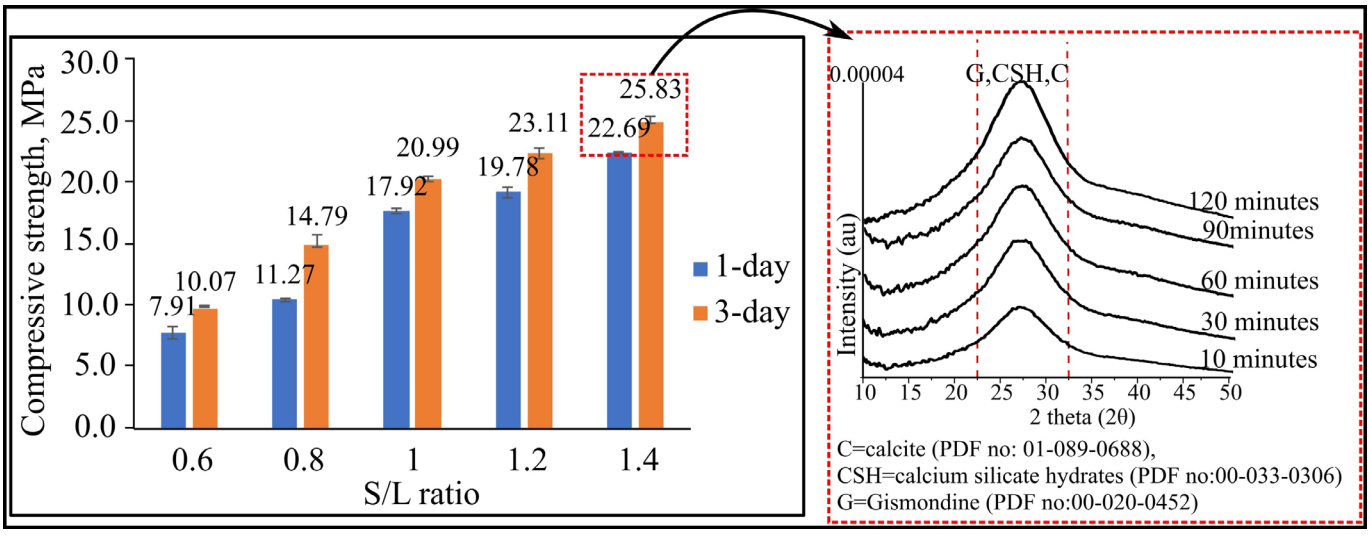

Fig. 4. Compressive Strength of Alkali-activated slag with Phase Evolution Analysis

ducing total cumulative heat evolved and contributing to greater strength performance. The results indicate that the nucleation kinetics could be employed as an indicator for comprehending the influence of the solid-to-liquid (S/L) ratio on strength performance. The high strength performance observed at the highest S/L ratio (1.4) is attributed to the increased availability of nucleation sites, the rapid growth rate, and the minimal cumulative heat evolved, resulting from the densified microstructure of alkali-activated slag.

5. Conclusions

From the findings obtained the following conclusion can be deducted:

- The findings obtained proved that the heat evolution can be potential for elucidating the nucleation kinetics with variation applied to the mix designation. Increasing in S/L ratios led to variation on the peaks of heat evolution thus attributing to the different in total cumulative heat evolved.
- The alkali activation process is governed by an instantaneous nucleation mechanism with one-dimensional rod-like growth, as confirmed by JMAK model analysis. The study highlights that increasing the S/L ratio enhances nucleation and polymerization rates, leading to improved compressive strength, with the highest strength recorded at an S/L ratio of 1.4. This improvement is attributed to the densification of polymeric networks and the phase evolution of calcium-hydrated products, which not only inhibit heat flow but also suggest the potential reutilization of evolved heat as an energy source for further polymeric bond formation. These findings provide valuable insights into optimizing alkali-activated slag systems for enhanced mechanical performance.

Limitations and Future Recommendations

This finding is significant in understanding the reaction and nucleation kinetics that lead to variations in the properties of alkali-activated slag. Therefore, further exploration of heat evolution is essential to gain a deeper understanding of the reactions occurring during the alkali activation process, with a particular focus on ambient curing, also referred to as self-curing in this study. Since self-curing does not require additional energy input, it offers a more sustainable approach for alkali-activated materials. Additionally, future research should emphasize monitoring the total cumulative heat evolved in other alkali-activated materials to mitigate thermal cracking issues in construction in which commonly occurred when dealing with alkali-activated slag. Excessive thermal cracking can significantly affect the durability and long-term performance of construction materials, making this an important area for continued investigation.

REFERENCES

[1] A. Bilginer, O. Canbek, S. Turhan Erdoğan, J. Mater. Civ. Eng. **32**, 04019316 (2020).
[2] Z. Jiao, Y. Wang, W. Zheng, W. Huang, Adv. Mater. Sci. Eng. **2018**, 10-12 (2018).
[3] F. Puertas et al., Cem. Concr. Compos. **85**, 22-31 (2018).
[4] S. Kumar, P.D. Gautam, B. Sarath Chandra Kumar, Int. J. Innov. Technol. Explor. Eng. **8**, 947-952 (2019).
[5] Z. Hu, M. Wyrzykowski, P. Lura, Cem. Concr. Res. **129**, 105971 (2020).
[6] S.K. Nath, S. Kumar, Adv. Powder Technol. **30**, 1079-1088 (2019).
[7] H. Alanazi, J. Hu, Y.R. Kim, Constr. Build. Mater. **197**, 747-756 (2019).
[8] W. Al Makhadmeh, A. Soliman, J. Sustain. Cem. Mater. **0**, 1-17 (2020).
[9] G. Furtos, D. Prodan, C. Sarosi, D. Popa, M. Moldovan, K. Korniejenko, Materials (Basel). **17**, 7 (2024).
[10] G.D.E. Schutter **25**, 593-604 (1995).
[11] Y. Ling, K. Wang, X. Wang, S. Hua, Constr. Build. Mater. **228**, 116763 (2019).
[12] L. Hou, J. Li, Z. yuan Lu, Constr. Build. Mater. **226**, 250-258, (2019).
[13] P. Chindaprasirt, T. Phoo-ngernkham, S. Hanjitsuwan, S. Horpibulsuk, A. Poowancum, B. Injorhor, Case Stud. Constr. Mater. **9**, e00198 (2018).
[14] K. Duan, Z. Liu, X. Li, D. Wang, W. Cao, Y. Zhao, J. Clean. Prod. **450**, October (2023).
[15] Q. Ren et al., Metals (Basel). **13**, 4 (2023).
[16] A. Cousture, N. Renault, K. Ndiaye, J. Gallias, C.Y. Cergy, P. Universit, Constr. Build. Mater. **441**, 137501 (2024).
[17] S.K. Nath, S. Mukherjee, S. Maitra, S. Kumar, J. Therm. Anal. Calorim. **127**, 1953-1961 (2017).
[18] K. Shirzad, C. Viney, J.R. Soc. Interface **20** ,203 (2023).
[19] A.A. Siyal, K.A. Azizli, Z. Man, L. Ismail, M.I. Khan, Ceram. Int. **42**, 15575-15584 (2016).
[20] T. Phoo-Ngernkham, C. Phiangphimai, N. Damrongwiriyanupap, S. Hanjitsuwan, J. Thumrongvut, P. Chindaprasirt, Adv. Mater. Sci. Eng. **2018** (2018).